Electronic Supplementary Information (ESI) for *Chem. Commun.*

Mechanically inducible fluorescence clolour switching in formation of organic nanoparticles of an ESIPT molecule

Hiroshi Yao* and Tomohito Funada

Graduate School of Material Science, University of Hyogo, 3-2-1 Koto, Kamigori-cho, Ako-gun, Hyogo 678-1297, Japan

yao@sci.u-hyogo.ac.jp

Excitation spectra of AHBT *composites*.

Fig. S1 shows the excitation spectra of AHBT *composites* prepared at $\rho = 1$ and 4 monitored at both 450 and 500 nm. The spectra were recorded on a Hitachi F-4500 spectrofluorometer.

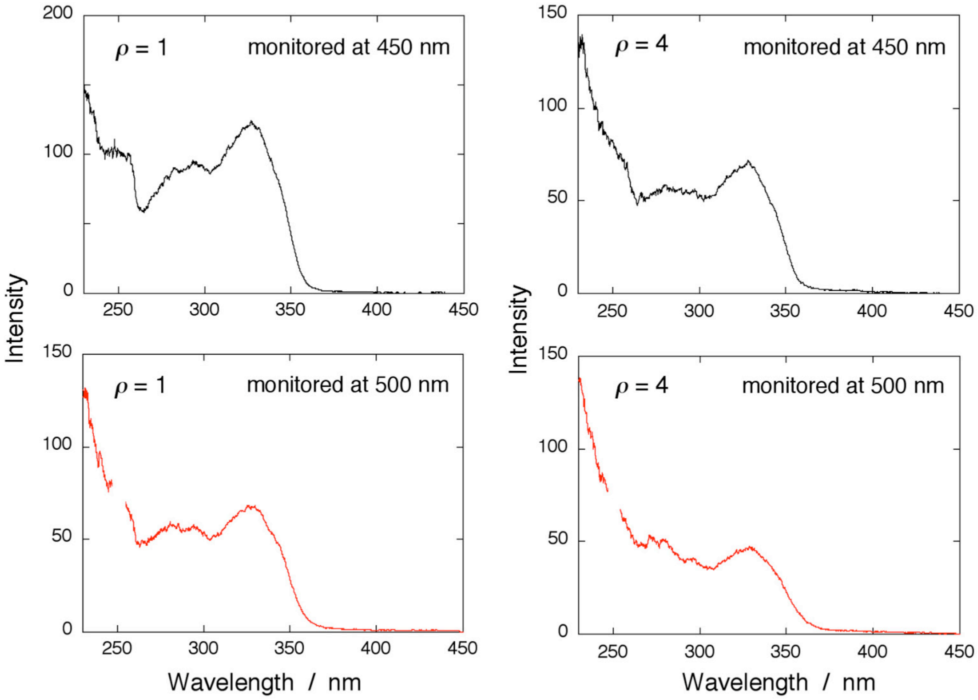

Fig. S1. Excitation spectra of the blue (450 nm) and green (500 nm) fluorescence of AHBT *composites* prepared at $\rho = 1$ and 4.

In all cases, the excitation spectra have peaks at around 328, 293, and 281 nm. The absorption spectra for the corresponding samples exhibited peaks at around 330, 293, and 280 nm, essentially identical with those in the excitation spectra. When we look more closely at these excitation spectra, interestingly, those monitored at 500 nm (that is, mainly keto emission) showed slightly broader spectral features compared to both the absorption and excitation spectra monitored at shorter wavelength (450 nm; enol emission). This indicates that the two emissive states are somewhat different from each other, and here the electrostatic interactions between AHBT$^+$ and TFPB$^-$ modulate the absorption spectral profiles[1] and thus should be responsible for the “green” keto emission.

Excitation spectra of AHBT *nanoparticles*.

Fig. S2 shows the excitation spectra of AHBT *nanoparticles* monitored at 450 and 580 nm. The *nanoparticle* samples were obtained through vigorous shaking of the corresponding *composite* solution with $\rho = 1$ and 4.

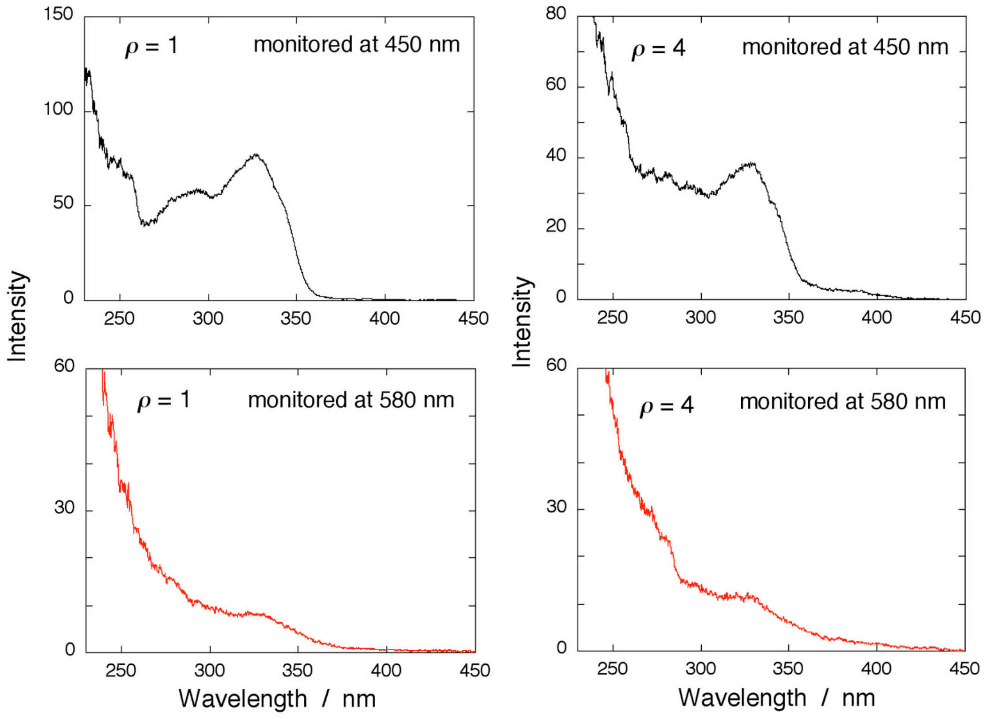

Fig. S2. Excitation spectra of the blue (450 nm) and yellow (580 nm) fluorescence of AHBT *nanoparticles* obtained through vigorous shaking of the corresponding composite solution for $\rho = 1$ and 4.

Clearly, the dual emission (enol and keto (ESIPT) emission at 450 and 580 nm, respectively) exhibits different excitation spectra, also indicating that the two emissive states are different from each other. Since the excitation spectrum of the *nanoparticle* sample ($\rho = 1$) monitored at 450 nm is almost identical with the absorption spectrum of AHBT in acetic acid solution, the enol emission comes from the protonated AHBT. It is interesting to note that, unlike the excitation spectra of the AHBT *composites* (keto emission) as shown in Fig. S1, appearance of a broad tailing profile at $\lambda \geq$ 350 nm accompanied by a large intensity decrease at 300–330 nm is remarkable, in agreement with the evolution observed in the absorption spectra. As described in the main text, the broad tailing at $\lambda \geq$ 350 nm can be ascribed to deprotonated (or neutral) AHBT chromophore, so in this case, the interactions between neutral AHBT and TFPB (precisely, "modified" TFPB brought about by mechanical shaking under acidic condition) should be responsible for the "yellow-orange" ESIPT emission.

Spectral simulation.

Absorption spectrum of AHBT *nanoparticles* obtained after vigorous shaking of the acidic AHBT-TFPB *composite* solution with $\rho = 1$ can be nearly expressed as a linear combination of the three absorption components; (i) free (or molecularly dispersed) AHBT in acetic acid solution, (ii) AHBT *nanoparticle* solution with $\rho = 4$, and (iii) hydrolyzed (= modified) TFPB in acetic acid solution. This means that, after vigorous shaking of the AHBT–TFPB *composite*, the solution contains these three components. Fig. S3a displays the absorption spectrum of AHBT *nanoparticles* ($\rho = 1$) reproduced by the above three spectral components. Fig. S3b represents comparison between the absorption spectra of pure (fresh) TFPB and hydrolyzed TFPB in acetic acid solution (pH ~3.3).

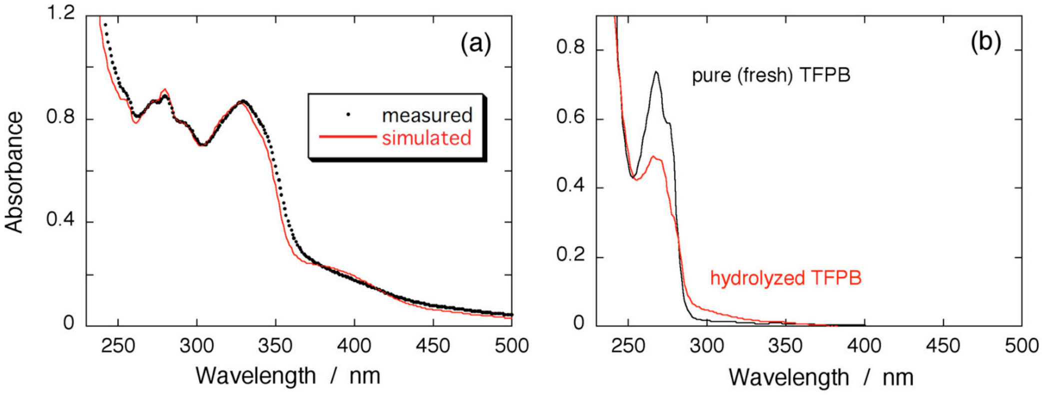

Fig. S3. (a) Absorption spectrum of the AHBT *nanoparticles* ($\rho = 1$; dotted curve) superimposed with the linear combination of three components (red solid curve). (b) Absorption spectra of pure (fresh) and hydrolyzed TFPB in acetic acid solution. The hydrolyzed TFPB was obtained by keeping the freshly prepared acetic acid solution containing TFPB for about two weeks in dark at room temperature.

Thermal stimulation induces formation of nanoparticles with keto emission.

The AHBT-TFPB *composite*, which was prepared by mixing AHBT and fresh TFPB in aqueous acetic acid solution (with PVP, $\rho = 4$), was heated at 70°C for 60 min. Figs. S4-a and S4-b show a set of UV-vis absorption and fluorescence spectra sampled at different times during the heating process. Upon heating of the solution, both the absorption and fluorescence spectra changed. The shape and peak positions for the spectrum sampled at 60 min are in agreement with those for the AHBT *nanoparticle* species synthesized via vigorous shaking. Therefore, thermal stimulation (or heating) has a similar effect to the mechanical shaking (in other words, mechanical shaking acts as local heating of the *composites*), which facilitates the formation of *nanoparticles* with keto emission and suggests a possibility of thermo-responsive fluorescence switching.

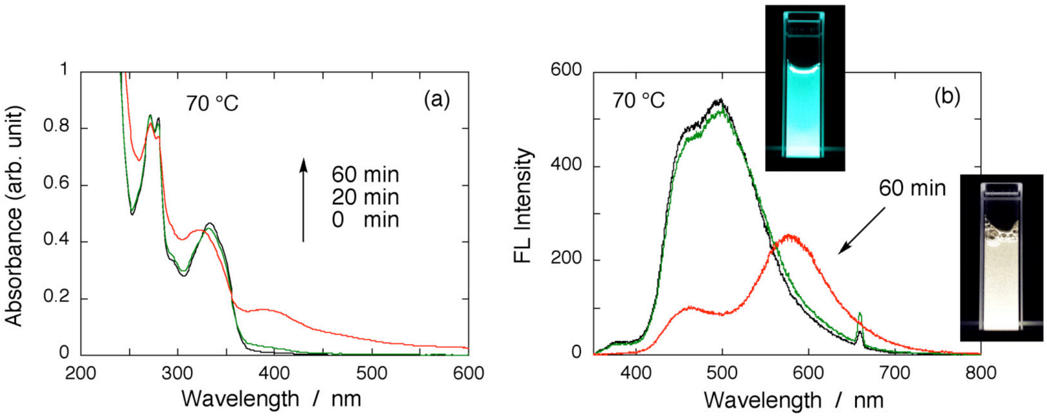

Fig. S4. (a) Absorption and (b) fluorescence spectra of samples ($\rho = 4$) evolved from the heating treatment at 70 °C. Black curves are for the AHBT-TFPB *composite* sample. Green and red curves are for samples taken at different times (20 and 60 min) of the heat treatment, respectively. Fluorescence images taken under 365 nm UV irradiation (20 and 60 min) are also shown.

IR absorption properties of TFPB and related compounds.

We focused on vibrational information on the several boron compounds that exhibit characteristic peaks in the 400–1800 cm^{-1} region. Figs. S5-a and S5-b show measured IR absorption spectra of pure (fresh) TFPB and “modified” (hydrolyzed) TFPB. Upon storage of the acidified TFPB solution for 1 day, we found several new IR peaks in addition to the original peaks that can be ascribed to pure TFPB. They are marked with red arrows in the figure; for example, appearance of new peaks at 831 and 1594 cm^{-1}, suggesting the hydrolysis of TFPB in acidified solution. The bands at around 800–850 and 1580–1600 cm^{-1} can be assigned to the out-of-plane C-H bending and the C-C stretch in the aromatic rings, respectively. Then the hydrolyzed product has higher energy of ~16 cm^{-1} for the C-C stretch vibration in comparison to that of pure TFPB.

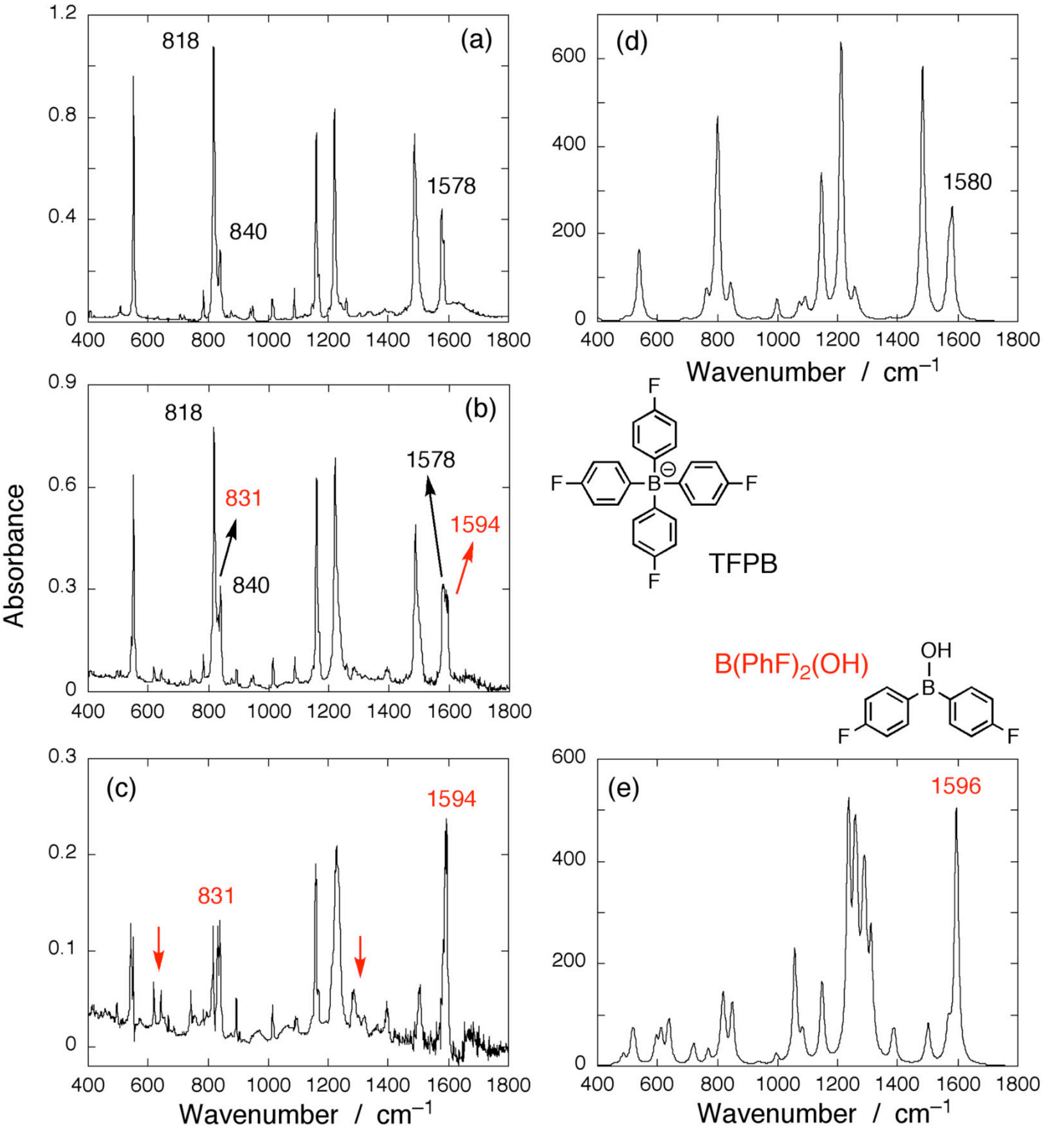

Fig. S5 (a) and (b) Measured IR absorption spectra of pure TFPB (NaTFPB) and "modified" (hydrolyzed) TFPB obtained after vigorous shaking. (c) Difference spectrum between pure (fresh) and "modified" TFPB. (d) and (e) Calculated IR absorption spectra of pure TFPB and bis(4-fluorophenyl)borinic acid B(PhF)$_2$(OH).

To clearly see the change in their spectral profiles, difference spectrum between Figs. S5-a and S5-b was calculated. The result is shown in Fig. S5-c. Note that subtraction factor was determined to avoid oversubtraction (that is, to avoid the presence of sharp negative values). According to Fig. S5-c, the band at 1594 cm^{-1} is prominent. Moreover, we found bands at 1300–1350 cm^{-1} that can be assigned to stretch modes of B-O, giving evidence of the borate hydrolysis. One approach for the determination of molecular structures from the spectroscopic IR data is to optimize the molecular geometry for possible low energy structures of the system using density functional theory (DFT), and for the optimized structures, to simulate the spectra. All calculations were performed with the DFT programs (B3LYP/6-31G*) provided by the Gaussian 09 suite.[2] Figs. S5-d and S5-e show calculated IR absorption spectra of TFPB and bis(4-fluorophenyl)borinic acid $B(PhF)_2(OH)$, the most probable candidate for the hydrolyzed (= modified) species. First, by comparing the spectra of Figs. S5-a and S5-d, the DFT calculations almost fully reproduced the IR spectrum of pure TFPB measured. We therefore are confident that the calculations can be successfully applied to study the energetics and IR spectra. We then compared the difference spectrum with that of calculation for $B(PhF)_2(OH)$. See Figs. S5-c and S5-e. From these spectra, the difference spectrum is in satisfactorily agreement with the calculated spectrum of $B(PhF)_2(OH)$, so this compound should be the counterpart that can interact with AHBT molecules in the *nanoparticles*.

MALDI-FOF MS of fresh and modified (hydrolyzed) TFPB.

Matrix-assisted laser desorption/ionization-time of flight mass spectrometry (MALDI-TOF MS) analysis was performed using a Voyager DE PRO system (Applied Biosystems), equipped with a N_2 laser source (337 nm). Mass spectra were acquired for negative ions in a linear mode. Samples for measurements were prepared by mixing fresh or hydrolyzed TFPB solution with the matrix (α-Cyano-4-hydroxycinnamic acid (CHCA), acetonitrile/acetic acid solution) and directly placed onto the stainless steel sample plate.

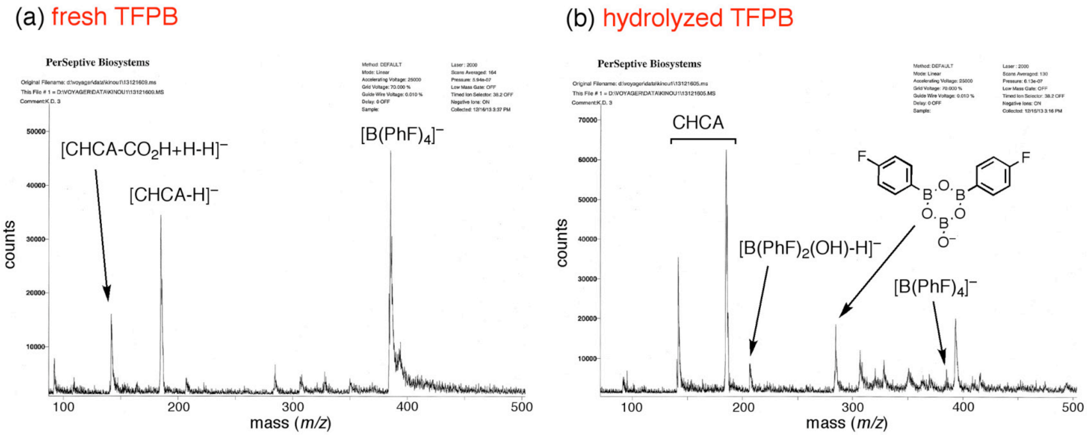
(a) fresh TFPB
(b) hydrolyzed TFPB

Fig. S6 Negative-ion MALDI mass spectra of (a) fresh TFPB and (b) hydrolyzed TFPB. Matrix peaks are labeled with “CHCA”.

Negative-ion MALDI mass spectra of fresh (pure) and hydrolyzed TFPB are illustrated in Fig. S6. For fresh TFPB (Fig. S6-a), an intact molecular ion peak (major peak) was observed at *m*/*z* 391. In the case of hydrolyzed TFPB (Fig. S6-b), the intact borate peak was significantly decreased whereas fragment peaks corresponding to the species of $B(PhF)_2O^-$ and $[B(PhF)O]_2BO_2^-$ were additionally observed, suggesting formation of diarylborinic acid and arylboronic acid (one form of anhydrides).[3] Since 4-fluorophenylboronic acid did not produce the AHBT-based *nanoparticles* (as shown in the main text), bis(4-fluorophenyl)borinic acid should be the most probable counterpart in the nanoparticle systems.

IR absorption spectrum of the AHBT-modified TFPB precipitate.

Mixing of AHBT and "modified" TFPB dissolved in acetic acid solution without PVP yielded a small amount of solid precipitate. We then isolated and purified the precipitate, and identified the product by the FT-IR measurement. Fig. S7 shows IR absorption spectra of the reactants AHBT and modified (hydrolyzed) TFPB along with that of the precipitate (or AHBT-modified TFPB adduct).

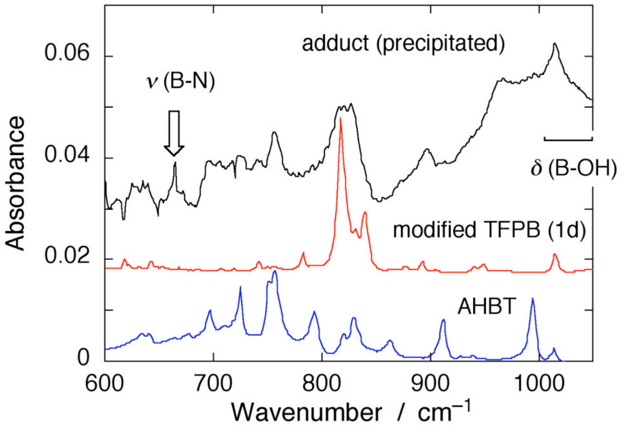

Fig. S7 IR absorption spectra of the AHBT-modified TFPB adduct (precipitate), modified (hydrolyzed) TFPB, and AHBT in the energy region of 600–1050 cm^{-1}.

In the IR spectrum of the solid-state adduct, it was reasonably composed of the respective counterparts. In addition, importantly, we found a new peak at ~660 cm^{-1} that can be assigned to the B-N stretch mode of amine-borane adducts,[4] suggesting the presence of B-N bond formation.

References

1 Z. Ou, H. Yao, K. Kimura, *Bull. Chem. Soc. Jpn.*, 2007, **80**, 295.

2 M. J. Frisch, G. W. Trucks, H. B. Schlegel, G. E. Scuseria, M. A. Robb, J. R. Cheeseman, G. Scalmani, V. Barone, B. Mennucci, G. A. Petersson, H. Nakatsuji, M. Caricato, X. Li, H. P. Hratchian, A. F. Izmaylov, J. Bloino, G. Zheng, J. L. Sonnenberg, M. Hada, M. Ehara, K. Toyota, R. Fukuda, J. Hasegawa, M. Ishida, T. Nakajima, Y. Honda, O. Kitao, H. Nakai, T. Vreven, J. A. Montgomery, Jr., J. E. Peralta, F. Ogliaro, M. Bearpark, J. J. Heyd, E. Brothers, K. N. Kudin, V. N. Staroverov, T. Keith, R. Kobayashi, J. Normand, K. Raghavachari, A. Rendell, J. C. Burant, S. S. Iyengar, J. Tomasi, M. Cossi, N. Rega, J. M. Millam, M. Klene, J. E. Knox, J. B. Cross, V. Bakken, C. Adamo, J. Jaramillo, R. Gomperts, R. E. Stratmann, O. Yazyev, A. J. Austin, R. Cammi, C. Pomelli, J. W. Ochterski, R. L. Martin, K. Morokuma, V. G. Zakrzewski, G. A. Voth, P. Salvador, J. J. Dannenberg, S. Dapprich, A. D. Daniels, O. Farkas, J. B. Foresman, J. V. Ortiz, J. Cioslowski, D. J. Fox, *Gaussian 09*, Gaussian, Inc., Wallingford CT, 2010.

3 D. Barriet, C. M. Yam, O. E. Shmakova, A. C. Jamison, T. R. Lee, *Langmuir*, 2007, **23**, 8866.

4 D. N. Reinemann, A. M. Wright, J. D. Wolfe, G. S. Tschumper, N. I. Hammer, *J. Phys. Chem. A*, 2011, **115**, 6426.